Environ Earth Sci (2017) 76:587
DOI 10.1007/s12665-017-6919-8

ORIGINAL ARTICLE

Multi-proxy records of Quaternary fluvio-lacustrine sediments around Lakes Eymir and Mogan, Ankara (Central Anatolia, Turkey)

Ceren Küçükuysal[1] · Nurdan Yavuz[2]

Received: 14 December 2016 / Accepted: 16 August 2017 / Published online: 24 August 2017

Abstract This paper presents the mineralogical, geochemical, palynological and stable isotopic compositions of the Late Pleistocene–Holocene fluvio-lacustrine sediments around Lakes Eymir and Mogan (Ankara), Central Anatolia. It is based on the interpretation of the multi-proxy records in conjunction with the geochronological data in eight different sections. The comparison between the increase/decrease in the abundances of carbonates and total clay assemblages is correlated with the changing abundance of coniferous forests and herbaceous plants (mainly Asteraceae and Chenopodiaceae). $\delta^{13}C$ and $\delta^{18}O$ values and molecular weathering ratios of the sediments revealing the hydrolysis, evaporation and leaching together with chemical index of alteration (CIA) provide insight into the climatic changes in the study area between 11,899 and 1428 cal year BP. Relatively higher total clay amount, $\delta^{18}O$ of around −8‰ and higher CIA (>40%) with higher hydrolysis suggest humid conditions during 11,899–6448 cal year BP. Between 6448 and 5763 cal year BP, sediments show oscillations between high and relatively low values of the proxy data implying intercalation of dry and wet seasons. The last period recorded between 5763 and 1428 cal year BP is realized with high calcite precipitation–low total clay and low CIA and relatively higher salinization which directly characterize aridity.

Keywords Mineralogy · Palynology · Stable isotope · Molecular weathering ratio · Gölbaşı

Introduction

The Holocene has become a very popular time span to develop systematic knowledge on the palaeoclimatic and palaeoweathering conditions by many different proxies from different geological settings (Landmann et al. 1996; Eastwood et al. 1999; Wick et al. 2003; Mayewski et al. 2004; Staubwasser and Weiss 2006; Kotthoff et al. 2008; Jalut et al. 2009; Peyron et al. 2011; Benito et al. 2015; Mauri et al. 2015). Among those, terrestrial records, especially fluvial and lacustrine evidences, have been employed widely for the palaeoclimatic reconstruction studies. Small changes in climatic systems may result in major changes in the geomorphological processes in the lake catchments, fluctuations in the lake level and sediments deposited within (Roy et al. 2009). Such changes may lead to variable mineralogical and geochemical changes; for this reason, they have been used as proxies to infer the palaeoenvironmental conditions of Quaternary terrestrial records. The clay mineralogy of the sediments can additionally provide proxy data which can be used in combination with the other proxies to reconstruct the climatic signals (Bischoff and Cummins 2001; Tamban et al. 2002; Yuretich and Ervin 2002; Jason et al. 2005; Diekmann et al. 2008; Martins et al. 2013; Altın et al. 2015; Veldkamp et al. 2015). Anatolia has become a popular

Electronic supplementary material The online version of this article (doi:10.1007/s12665-017-6919-8) contains supplementary material, which is available to authorized users.

✉ Ceren Küçükuysal
cerenkucukuysal@mu.edu.tr

[1] Geological Engineering Department, Muğla Sıtkı Koçman University, Kötekli, Muğla, Turkey

[2] Geological Research Department, General Directorate of Mineral Research and Exploration (MTA), Üniversiteler Mahallesi, Dumlupınar Bulvarı No. 139, 06800 Çankaya, Ankara, Turkey

region for the palaeoclimate studies and has been widely investigated archaeologically, geologically, geomorphologically and limnologically in recent years (e.g. Kuzucuoğlu et al. 1998; Kazancı et al. 2004, 2012; Doğan 2010; Göktürk et al. 2011; Ocakoğlu et al. 2013; Eriş 2013; Kuzucuoğlu et al. 2011; Şenkul and Doğan 2013; Arıkan 2015; Benito et al. 2015; Biltekin et al. 2015; Yavuz et al. 2016). Among such studies, terrestrial records from Central Anatolia have been evaluated in terms of Plio-Quaternary climates (e.g. Roberts 1983; Roberts and Wright 1993; Karabiyikoğlu et al. 1999; Çiner 2004; Doğan 2011; Jones et al. 2006; Kadir et al. 2013; Göz et al. 2014; Küçükuysal 2011, 2016; Küçükuysal et al. 2013; Küçükuysal and Kapur 2014; Altin et al. 2015; Yavuz et al. 2016). However, there is surprisingly no such evaluation on the Quaternary sediments around Lakes Mogan and Eymir, Ankara. Therefore, this study aims to present the first radiocarbon age data associated with the mineralogy, palynology and stable isotopic analysis of the fluvio-lacustrine sediments around Lakes Mogan and Eymir to provide better understanding of the local palaeoenvironmental conditions during the Late Pleistocene–Holocene. Furthermore, the presented data are compared with the recent findings in a regional sense to reveal possibility of correlation among the proxy data. The documented data will help to reconstruct the Quaternary climates of the study area for further detailed studies.

Description of the study area

The terrestrial records of the studied sections were selected from Central Anatolia (Fig. 1a, b). Lakes Mogan and Eymir are located in close vicinity of Ankara, almost 20 km south of the city (Fig. 1a). The lakes were previously part of the same fluvial system but then set by alluvial deposits and started to behave as two separate lakes. The Neogene stratigraphic sequence that exposed around these two lakes has fluviatile sediments with predominant lithologies consisting of reddish–brownish mudstones with immature to semi-mature calcrete occurrences. Calcretes are usually in the nodular, tubular, powdery and massive forms (Küçükuysal 2016). The physical appearances and macromorphological characteristics of these calcretes are revealed in Küçükuysal (2016) as quite similar with those in Bala (Küçükuysal et al. 2013) and in Karahamzalı (Küçükuysal and Kapur 2014). The reddish mudstones are supposed to be subjected to high leaching leading to the formation of nodular calcretes; however, the brownish mudstones are much enriched in powdery calcretes in immature stage.

The geology of the study area was studied in detail by Akyürek (1981) and Akyürek et al. (1979a, b, 1980, 1997) (Fig. 1). The oldest unit in the study area is the Early Triassic Emir Formation which consists of muscovite–quartz schist, sericite–chlorite–quartz schist, sericite–chlorite schist, phyllite, calcschist, meta-volcanics and meta-conglomerate. It is overlain by the Early–Late Triassic Elmadağ Formation which is composed of meta-conglomerate, meta-sandstone, sandy limestone, sandstone, limestone, agglomerate and meta-volcanics. It, in turn, is overlain by the Middle–Late Triassic İmrahor Limestone Member. Upcoming geological units in the younging direction are Permian limestone blocks and Miocene Hançılı Formation. The Hançılı Formation consists of clayey limestones, marl, siltstone, sandstone, conglomerate, gypsum, shale and some volcanics such as andesite, dacite and trachy-andesite. All of these sequences are succeeded by the Neogene clastics of Gölbaşı Formation which is composed of conglomerate, sandstone and mudstone. The youngest unit in the study area is the Quaternary alluvium deposits.

The modern climate conditions in the basin refer to continental climate, dominantly very cold and rainy/snowy days in winter but very hot and dry weather in summer. According to Yağbasan (2007), the arithmetic average of the annual precipitation in the basin is 333.9 mm and the annual average evaporation is 1092.2 mm. Therefore, with respect to the modern climatic conditions, the basin can be defined as a semi-arid region in terms of precipitation and is dominated by steppe-type vegetation cover.

Materials and methods

From different sites within the study area, eight sections (E-16, E-18, E-19, E-22, E-23, E-25, E-26 and E-4r) were selected and sampled in terms of mineralogical, palynological and stable isotope analyses (Fig. 2). Munsell colours (MC) of each section were recorded. The samples were mostly selected from mudstones in approximately every 10 cm throughout the sections. The top of all mudstones was covered by recent soil with modern vegetation. E-16 section is 235-cm-long mudstone section with 7.5 YR 4/4 Munsell colour. It shows almost homogenous structure with immature carbonate encrustations in the middle of the section (Fig. 2). E-22 section (mudstone with 10 YR 3/6 MC) is physically quite similar to E-16 section in calcrete occurrences. Totally 122-cm-long mudstone with blocky structure is recognized in this section. E-23 section is a 270-cm-long section enriched in carbonate coatings and shows 10 YR 7/4 MC. E-18 section (180 cm) has semi-mature carbonates at the top and at the bottom parts (7.5 YR 3/6 MC). E-4r section is a 265-cm-long section with 10 YR 5/2 MC. In the middle parts of E-4r section, carbonates are enriched in immature forms and a total of 24 samples

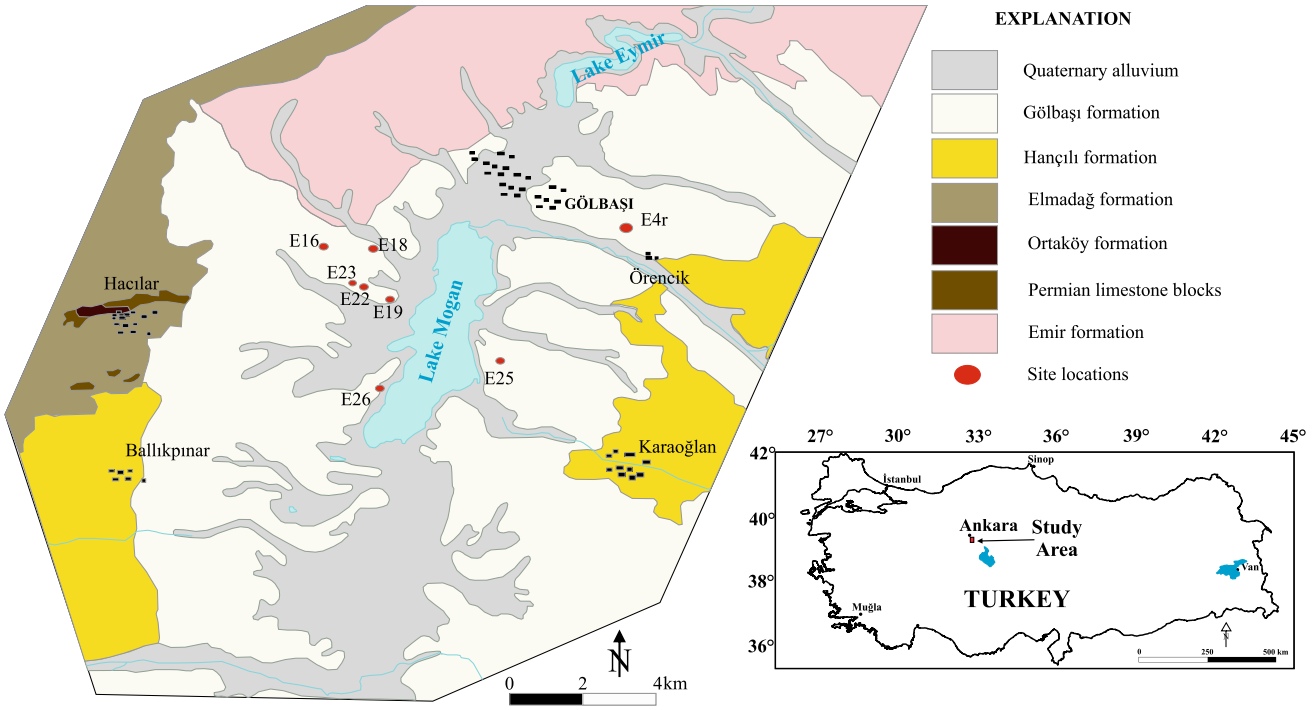

Fig. 1 Geological map of the study area showing the site locations (Akyürek et al. 1997). *Inset* shows the location of the study area in Turkey

were taken from this section. E-26 section is 135-cm-long mudstone section (10 YR 3/2 MC) with subangular blocky appearance. E-25 section (2.5 YR 4/4 MC) with 257-cm thickness presents blocky structure with immature carbonate concretions. E-19 section is a 150-cm-long section with 7.5 YR 3/4 MC, and 12 levels were sampled from this section.

Mineralogical compositions of the samples studied were determined by Bruker D8 Advance X-ray diffractometer (XRD) Cu target from 2° to 70° (2θ) for bulk powder samples and 5°–25° (2θ) for clay fraction (<2 μm). Combined procedures of Brindley (1980), Jackson (1979), Moore and Reynolds (1989), Thorez (1976) and Tucker (1988) were followed during the preparation of the oriented slides for X-ray diffraction. The relative abundances of minerals from the bulk sediments were estimated from the height of the main peak multiplied by the correction factors proposed by Gündoğdu (1982). To separate the clay fraction, samples were decarbonated with HCl first and finer than 2-μm fraction was separated by sedimentation procedure according to Stoke's law. The separated <2-μm size fraction was then mounted as oriented aggregates on glass slides (Moore and Reynolds 1997). For each sample, four X-ray patterns were recorded as air-dried (N), ethylene–glycol solvated for 24 h (EG) and heated at 350 and 550 °C for 2 h. Semi-quantitative estimations of the main clay minerals were obtained on EG diffractograms according to the methods of Biscaye (1965). The major elements were measured in Rigaku RIX 3000 wavelength-dispersive X-ray fluorescence (XRF) spectrometer. Stable isotope analysis ($\delta^{18}O$ and $\delta^{13}C$) of carbonates was carried out at Environmental Isotope Laboratory in University of Arizona. They were measured using an automated carbonate preparation device (KIEL-III) coupled to a gas-ratio mass spectrometer (Finnigan MAT 252). Powdered samples were reacted with dehydrated phosphoric acid under vacuum at 70 °C. The isotope ratio measurement is calibrated based on repeated measurements of NBS-19 and NBS-18, and precision is ±0.1‰ for $\delta^{18}O$ and ±0.08‰ for $\delta^{13}C$ (1 sigma). Radiocarbon ages of the samples were determined in Beta Analytical Inc., Miami, Florida, USA, using accelerator mass spectrometry. Samples for palynological analysis (ca. 20 g) were taken every 10 cm throughout the sections whenever organic-rich clays are available. Samples were treated with cold HCl (35%) and HF (70%) to remove carbonates and silica, followed by separation of the organic residue by means of $ZnCl_2$. The residue was sieved at 10 μm using a nylon mesh, mixed with glycerine and mounted on microscope slides. Counting was performed at 400× magnification using a Nikon Eclipse-Ni transmitted light microscope to a minimum pollen sum of 200 terrestrial pollen grains. Fossil pollen was identified using published keys (Faegri and Iversen 1989; Moore et al. 1991) and pollen atlases (Reille 1992; Stuchlik 1994). The palynological results shown in detailed pollen diagrams are obtained by using the programmes TILIA and TILIA GRAPH (Grimm 2005).

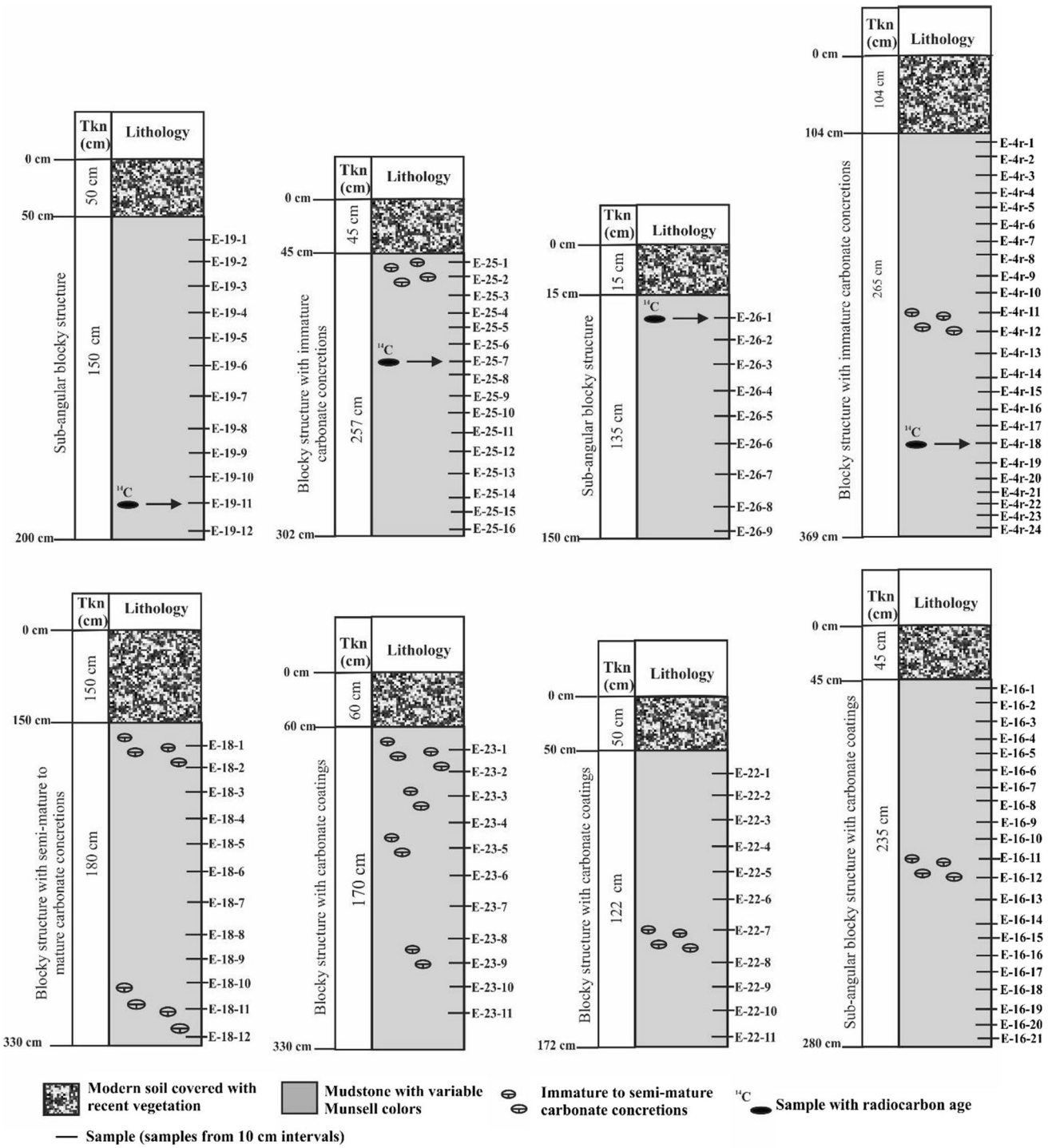

Fig. 2 Measured sections with depth, thickness, lithology, sample locations and radiocarbon age points

Results

Mineralogy

Mineralogical compositions of the samples were determined in terms of the major reflections, and the results of the semi-quantitative analysis are listed in Table S1. Quartz was determined by the presence of two prominent peaks at 0.427 and 0.334 nm. Feldspar, however, was identified by the most intense peak at 0.319 nm. A sharp and intense peak at 0.303 and 0.289 nm indicates the presence of calcite and dolomite, respectively. Smectite, the dominant

clay mineral found in the sections, was characterized by its basal reflection 1.4 nm which shifts to 1.7 nm by ethylene glycol solvation. Illite was identified by its characteristic peaks of 1.00 and 0.5 nm. The disappearance of the 0.715 nm peak after the heat treatment (550 °C) indicates the presence of kaolinite. Additionally, weak intense peaks in the 1.04–1.06 nm region may be related to the presence of palygorskite, and it requires further SEM–EDS analysis to have certainty on the presence.

The samples from the E-16 section reveal that total clay is the main mineral assemblage with an average abundance ranging around 58–67%. Calcite is the second most abundant one ranging from 14.7 to 22.9%, followed by the dolomite (4.5–8.6%) and feldspar (1.9–7.3%). The relative weight percentages of total clay, quartz, calcite and dolomite show almost similar variations. The clay fraction of the samples is composed dominantly of smectite, illite and kaolinite.

E-18 section, basinward to Lake Mogan than E-16, has the same mineral assemblages with E-16 except the absence of dolomite. Calcite is the only carbonate minerals found in this section with an average abundance of 6.13–35.4%, while total clay is the most abundant mineral ranging between 42.2 and 72.9%. The abundance of feldspar (3.7–23.3%) and quartz (11.4–27.04%) is relatively higher than those in E-16 section. Smectite and illite are the highly abundant clay minerals throughout the section.

In E-19 section, total clay is the dominant mineral phase with abundances between 33 and 60% through the section. It is followed by the presence of calcite (16–33%) and quartz (10–26%) and the absence of dolomite in the whole section. Total clay shows slight decreasing from bottom to sample E19-8 and starts to increase upwards of the section. Almost reverse variation between total clay and calcite is recognized in this section.

As in the previously mentioned sections, section E-22 is also characterized by the dominance of clays (14–34%) associated with high abundance of feldspars (9–43%) and calcite (18–64%) followed by relatively low amount of quartz (5–22%). The relative abundances of all minerals show good covariance with each other.

E23 section is composed of highly variant minerals of clays (24–56%), feldspar (18–62%), quartz (9–31%) and calcite (1–6%). Clay minerals are enriched in the middle of the section and show slight increase towards the top with the same trends in calcite, while the quartz amount lowers upwards in the section.

For section E-4r, the total clay abundance ranges from 33 to 74%, while feldspar also varies in a wide range of 13–44%. Calcite and quartz are also recognized with weight percentages of 1–12 and 7–22%, respectively. The most prominent trend is the reverse relationship between total clay and calcite in E-4r section.

E-25 section also shows the same pattern with E-4r having the reverse relationship between total clay (54–85%) and calcite (1–40%). Feldspar abundance varies between 2 and 11%, while the amount of quartz changes within a narrower range of 3–9%.

The last section, E-26, has consistency in the relative amounts of the minerals present. Total clay (30–39%), feldspar (18–32%), calcite (22–32%) and quartz (10–13%) are associated with the presence of dolomite ($\sim$2%).

Major element geochemistry

The major element data are presented as weight percentages of oxides and given in Table S2. In E-16 section, the major elements are almost constant all through the section. SiO_2, Al_2O_3, Fe_2O_3, MgO, CaO, Na_2O, K_2O, TiO_2, P_2O_5 and MnO vary in narrow range from bottom to top of the section. High MgO content ($\sim$5%) is directly associated with the presence of dolomite (Table S2). In section E-18, the situation is little different. SiO_2, Al_2O_3, CaO and Na_2O show relative enrichments at the same levels where the relative abundance of calcite and feldspar minerals is higher, while Fe_2O_3, MgO, K_2O, TiO_2, P_2O_5 and MnO are almost constant all through the section implying the presence of almost constant amount of smectite and illite (Table S2). In section E-22, CaO is relatively more abundant where calcite is also abundant. The decrease in SiO_2, Al_2O_3, Fe_2O_3, MgO, NaO, TiO_2 and K_2O is associated with the absence and/or decrease in amount of feldspar and smectite contents (Table S2). In section E-23, high amounts of SiO_2, Al_2O_3, Na_2O and K_2O are directly related to the high content of feldspar and smectite in the samples. Very low amount of CaO through the section is directly related to the accessory amount of calcite mineral present in all samples of E-23 (Table S2).

Molecular weathering ratios are estimated using major element data (Retallack 1997, 2001; Sheldon and Tabor 2009) to assign the conditions of geochemical processes of clayeyness, salinization and calcification (Table 1). Additionally, chemical index of alteration (CIA) values is evaluated to understand the weathering intensity of feldspars and their hydration to clay minerals (Table 1). Salinization is the process by which mobile elements (K and Na) accumulate as soluble salts (Sheldon and Tabor 2009). Calcification is another process related to the enrichment of CaO and MgO relative to Al_2O_3. (Al_2O_3/K_2O) is given as a measure of clayeyness since Al accumulates in clay minerals while K is deposited in silicates mostly. Base loss ratio is also used as leaching indicator where the abundance of base elements is divided into TiO_2 which is assumed to be more constant relative to the other mobile ones (Retallack 1997, 2001; Sheldon and Tabor 2009).

Table 1 Formulas of molecular weathering ratios and chemical index of alteration (Retallack 1997, 2001; Sheldon and Tabor 2009)

Process	Molar ratio	Indicator	Normal value	Strong effect
Salinization	$(K_2O + Na_2O)/Al_2O_3$	Hydrolysis	<1	>1
Calcification	$(CaO + MgO)/Al_2O_3$	Evaporation	<2	>10
Clayeyness	Al_2O_3/SiO_2	Hydrolysis	0.1–0.3	>0.3
Base loss	Base/Ti	Leaching	<2	>100
CIA	$Al_2O_3 \times 100/(Al_2O_3 + Na_2O + CaO + K_2O)$	Alteration	~2	>10

In section E-16, the molecular weathering ratios and CIA values are shown in Fig. 3a. Salinization is lower than 1 which points the average climatic conditions favouring low salinization; it is only relatively higher at the middle part of the section which is also correlated with the high calcification values. Clayeyness is almost stable all through the section with 0.21–0.24 values pointing normal conditions. Calcification is almost greater than 2, showing moderate calcification (Table S3). Base loss varies within a narrow range around 2. CIA is between 32 and 38% pointing low to moderate alteration degree for section E-16. The highest CIA values coincide with the lowest calcification and total base amount. This is the wet condition leading to high alteration with loss of Ca, Mg, Na and K.

In section E-18, the calculated molecular weathering ratios and the CIA values are plotted versus depth (Table S3). Salinization is generally less than 1, showing normal conditions with low salting. Towards the top of the section, there is a slight enrichment in salinization value. Calcification fluctuates between values of 1 and 3 showing low to moderate calcification degrees. Clayeyness is almost constant and lower than 0.20 which is a normal condition. Base loss is very similar to calcification and shows

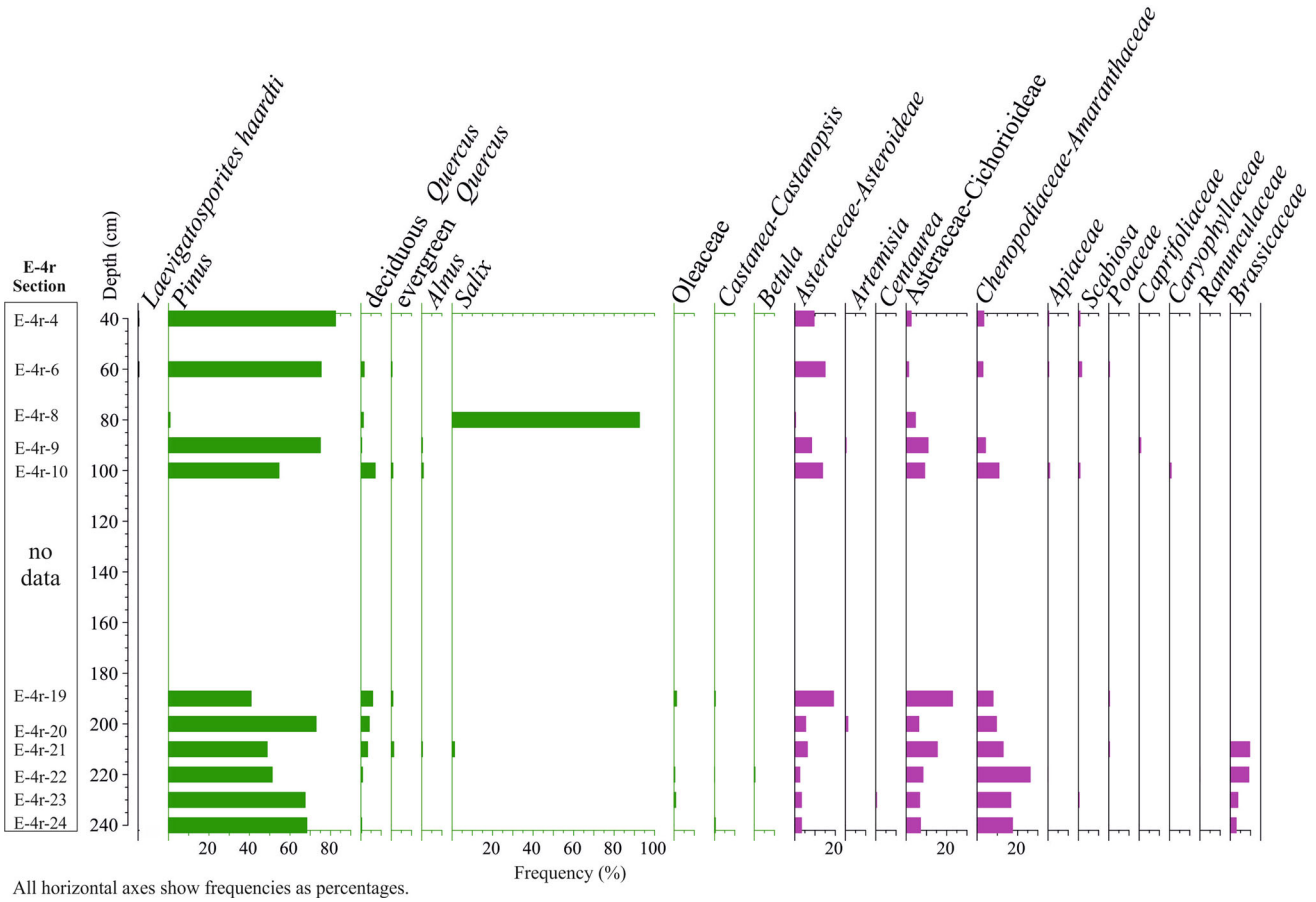

Fig. 3 Percentage pollen diagram of the E-4r section. In *green* are the trees and tall shrubs, in *fuschia* the herbs and xerophytes

fluctuations from 1 to 3. CIA is around 50% which points moderate alteration. The high calcification and base loss values are directly on the low CIA point, implying dry conditions. On the other hand, the lower calcification and base loss values coincide with the high CIA values, pointing dry conditions.

In section E-22 (Table S3), salinization decreases towards the top of the section from 2 to 0.5, from moderate to low salting conditions. Calcification is almost constant with two exceptions on sample E-22-3 and sample E-22-10 where its value reaches to 6 and almost 10. Clayeyness is on the other hand plots an opposite trend to salinization and shows an increase towards the top. Base loss trend is also parallel to calcification, and at the same two points, it shows high values. CIA is between 10 and 40, which means low to moderate alteration degrees. Samples E-22-3 and E-22-10 with high calcification and total base with low CIA values point dry conditions.

In section E-23 (Table S3), salinization is around 2 which is relatively higher salinization condition. Calcification is also almost constant with just one enrichment in E-23-3 sample where total base amount is also high. Clayeyness fluctuates within a narrow range between 0.16 and 0.20. CIA is higher than 55% and reaches to almost 70% which directly points moderate to high alteration degrees. The low degree in CIA is also correlated with the higher calcification pointing dry condition.

The degree of chemical weathering in soils increases with mean annual precipitation (P; mm) and mean annual temperature (T; °C) (Kovacs et al. 2013). According to Sheldon et al. (2002), mean annual precipitation (MAP) can be related to the chemical index of alteration without potassium (CIA − K) as geochemical climofunction and is calibrated for precipitation values between 200 and 1600 mm/year:

$$\mathrm{MAP\,(mm/year)} = 14.265(\mathrm{CIA} - \mathrm{K}) - 37.632$$

where $\mathrm{CIA} - \mathrm{K} = 100 \times [\mathrm{Al_2O_3}/(\mathrm{Al_2O_3} + \mathrm{CaO} + \mathrm{Na_2O})]$ (Kovacs et al. 2013). Results obtained from the studied samples are listed in Table S3 and as follows: for section E-16, the calculated average MAP value is 499 mm/year. The MAP values are stable all through the section. In section E-18, the calculated average MAP is 614 mm/year where the values are fluctuating from 335 to 939 mm/year through the section. It is relatively lower in section E-22 where the average MAP is 288 mm/year and the whole data range from 98 to 505 mm/year. The highest calculated average MAP is observed in section E-23 as 922 mm/year. The section is assumed to experience almost stable precipitation with very close precipitation values in a narrow range.

Stable isotope data

Stable isotope data are widely preferred in palaeoclimatology studies since they are accepted as good proxies reflecting changes in environmental conditions. The stable isotopic ratios of oxygen and carbon from carbonates can record changes in climatic conditions and plant cover. The stable isotope compositions of the samples studied were measured relative to standards, Vienna Pee Dee Belemnite (VPDB). They are expressed with delta notation (δ) in parts per thousand (‰ or per mille) (Table S4).

The isotopic composition of sediment carbonates in E-18 exhibits wide range in $\delta^{13}C$ values from −3.38 to −11.08‰ and in $\delta^{18}O$ from −5.16 to −9.63‰. The isotope values of sediment carbonates in E-4r section, like E-18 samples, display wider range for $\delta^{13}C$ from −5.80 to −13.02‰ and relatively narrower range for $\delta^{18}O$ from −7.07 to −8.90‰. This corresponds to the vadose zones which are characterized by large variations in the $\delta^{13}C_{carb}$ record and rather constant, but negative $\delta^{18}O_{carb}$ values due to subaerial exposures (Oehlert and Swart 2014). On the other hand, the samples from section E-22 display relatively narrower range in $\delta^{13}C$ from −5.87 to −7.79‰ and in $\delta^{18}O$ from −7.04 to −7.65‰. It is almost the same case for section E-16. The $\delta^{13}C$ values range from −7.03 to −8.33‰, and $\delta^{18}O$ values range between −5.51 and −6.34‰.

Radiocarbon ages

This study is the first to give radiometric ages of the Quaternary units around Lake Mogan and Eymir, Central Anatolia. Four samples from the studied area were employed for radiocarbon dating by accelerator mass spectrometer (AMS) in BETA Analytic Inc. The samples and their laboratory codes are provided together with the measured radiocarbon ages and calibrated ages in Table 2. Radiocarbon dating method (herein referred to as RC) is highly employed technique for Quaternary materials. Two-sigma calibrated dates of the samples are used comparatively in this study to provide chronological framework for the interpretation, because pedogenic and/or groundwater processes can overprint the ages by multiple intervals of dissolution–reprecipitation yielding RC ages that provide an average value of all crystals present in the fraction (Deutz et al. 2001). It is well understood that the sediments around Lake Mogan and Eymir measured for this study are younger than the Late Pleistocene, most possibly presenting Late Pleistocene–Holocene transition.

Table 2 AMS dating results of the selected samples from this study

Sample data	Laboratory code	Measured age (BP)	Calibrated age (cal BP)
E-19-11	Beta-338287	5660 ± 30	6448 ± 29
E-25-7	Beta-338288	5000 ± 30	5763 ± 80
E-26-1	Beta-338289	1520 ± 30	1428 ± 53
E-4r-18	Beta-338284	10,200 ± 40	11,899 ± 128

Palynology

The palynological analysis of the very late Pleistocene–Holocene successions from Central Anatolia has been carried out on the samples of the sections E-4r, E26 and E24 (Figs. 3, 4). The microphotographs of some pollen grains identified from studied samples are shown in Fig. 5.

The section E-4r is characterized by the dominance of *Pinus* (52–83%). *Quercus* occurs as both evergreen subtropical species and deciduous temperate species. Deciduous *Quercus* slightly increases upward (max. 7%), while evergreen *Quercus* has a more uniform representation with an average of 1%. *Alnus*, *Betula*, *Castanea–Castanopsis* and Oleaceae are all represented by low percentages. *Salix* is present only in two samples but shows a maximum of 93%. Herb pollen is represented mainly by Asteraceae–Asteroideae (from 1 to 15%), Asteraceae–Cichorioideae (from 15 to 23%) and Chenopodiaceae/Amaranthaceae (from 3 to 26%). Asteraceae–Asteroideae increases upward, while Asteraceae–Cichorioideae and Chenopodiaceae/Amaranthaceae show a decreasing upward trend. Apiaceae, Poaceae, Caryophyllaceae, Caprifoliaceae, Ranunculaceae, Brassicaceae and *Scabiosa* constitute other herbs represented by lower percentages (1–9%) (Fig. 3).

Section E-24 is characterized by the co-dominance of *Pinus* (from 14 to 63%) and Chenopodiaceae/Amaranthaceae (from 30 to 73%). At lower parts of the section, *Pinus* increases, while Chenopodiaceae/Amaranthaceae decreases. However, in the rest of the section they show a steady presence, each around 35%. *Salix, Castanea–Castanopsis* and deciduous *Quercus* participate with frequencies below 3%. Asteraceae–Asteroideae and Asteraceae–

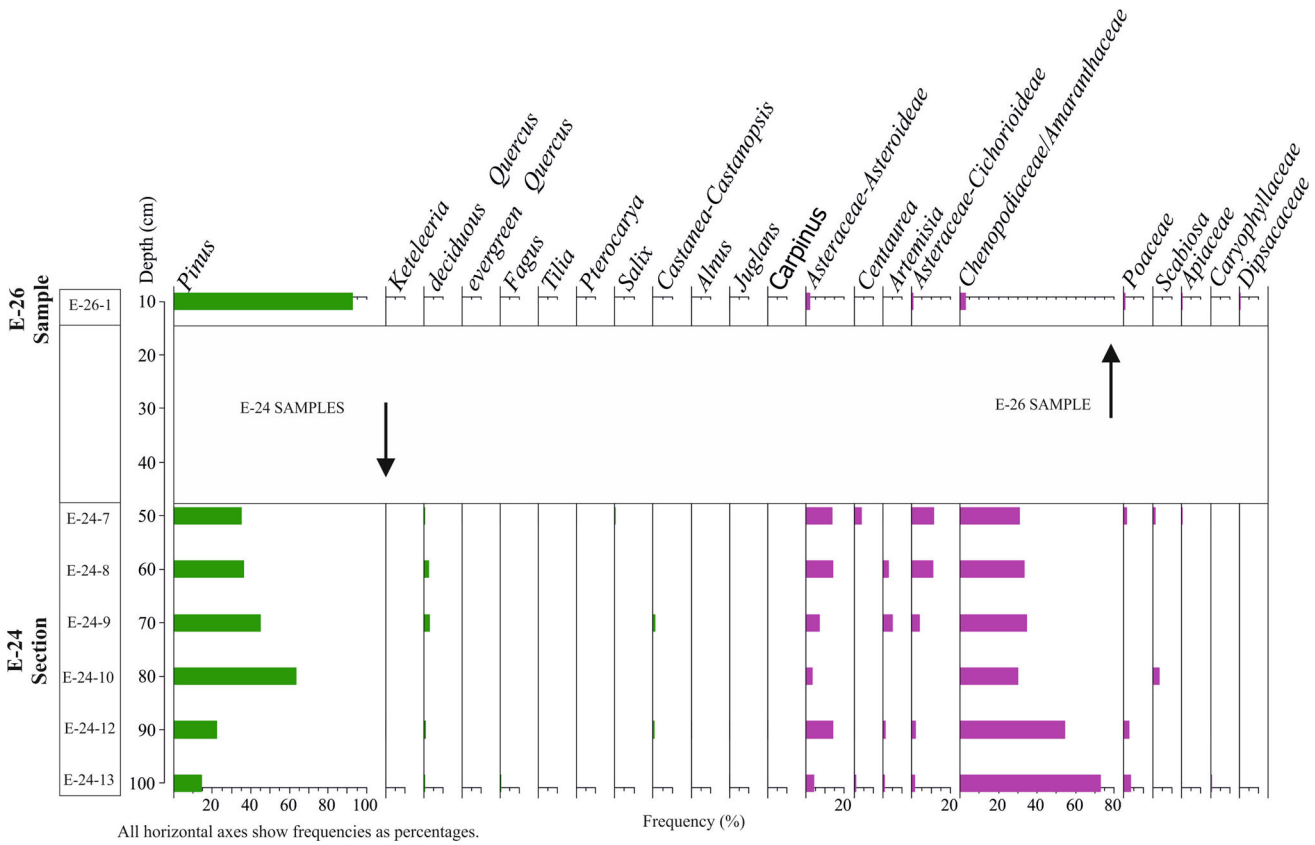

Fig. 4 Percentage pollen diagram of the sections E-24 and E-26. Note that the distance between samples is not at scale. In *green* are the trees and tall shrubs, in *fuschia* the herbs and xerophytes

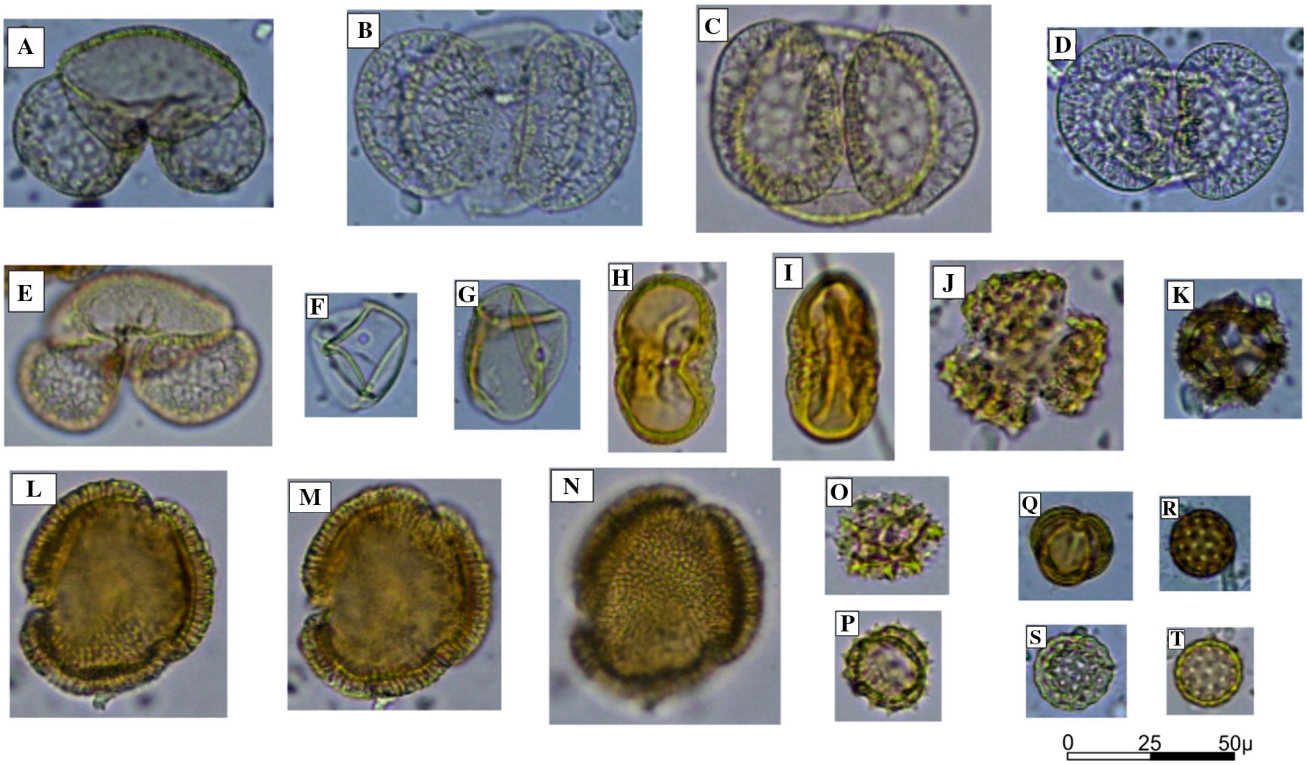

Fig. 5 Photographs of various pollen grains from the studied area (**a**–**e** *Pinus*, **f**, **g** *Poaceae*, **h**, **i** *Apiaceae*, **j**, **p**. Asteraceae–Asteroideae, **k**, **o** Asteraceae–Cichorioideae, **r** *Artemisia*, **s**–**u** Chenopodiaceae/Amaranthaceae)

Cichorioideae slightly increase upward (2–13%). *Artemisia* ranging from 1 to 5% is also well represented. Poaceae, *Scabiosa*, Apiaceae and Caryophyllaceae are represented by lower percentages (Fig. 4).

The only one sample from section E-26 is characterized by the predominance of *Pinus* with 93%. The rest is represented by very lower percentages of *Juglans*, Asteraceae–Asteroideae, Asteraceae–Cichorioideae, Chenopodiaceae/Amaranthaceae, Poaceae, Apiaceae, Caryophyllaceae and Dipsacaceae (Fig. 4).

Interpretation of the proxy records

The mineralogical, geochemical, isotopical and palynological data are interpreted here to infer the climatic conditions recorded during very Late Pleistocene–Holocene in Gölbaşı (around Lakes Mogan and Eymir), Central Anatolia. The reddish and brownish colours of the fluvio-lacustrine sediments around Lakes Mogan and Eymir are quite similar with those of Bala, Central Anatolia (Küçükuysal et al. 2013) and Karahamzalı, Central Anatolia (Küçükuysal and Kapur 2014). Calcretes are common in fluvio-lacustrine sediments studied, in nodular, powdery and massive forms which strongly suggests that they do not originate from rooting (Candy et al. 2003; Eren et al. 2008; Küçükuysal and Kapur 2014; Veldkamp et al. 2015) or cyanobacteria (Rabenhorst et al. 1991; Verrecchia et al. 1995; Wagner et al. 2012; Veldkamp et al. 2015) but pedogenesis and groundwater effect. The macro- and micro-morphology of the Late Pleistocene calcretes (MAP less than 50 mm/year) found in the fluvio-lacustrine sediments in the study area strongly suggests that the calcretes were formed under relatively arid conditions (Küçükuysal 2016).

Mineralogical abundances of the fluvio-lacustrine sediments around Lakes Mogan and Eymir reveal the inverse relationship between total clay and calcite (Fig. 6), suggesting humid climates with high degree of weathering are intercalated with dry climates associating with less intense weathering. Calcite precipitation is associated with high water and low rate of evaporation, while dolomite precipitation relates with low water level and high evaporation (Landmann et al. 1996; Altın et al. 2015). It is also stated by Ülgen et al. (2012) that an increase in the total clay amount indicates a high degree in chemical weathering and high humidity, while the reverse condition points drier climates with dominant physical weathering. In section E-25, this relation is clearly observed. The upper portion of the section younger than 5763 ± 80 cal year BP has the total clay abundances ranging between 50 and 70%, while the calcite has relatively higher percentages implying drier

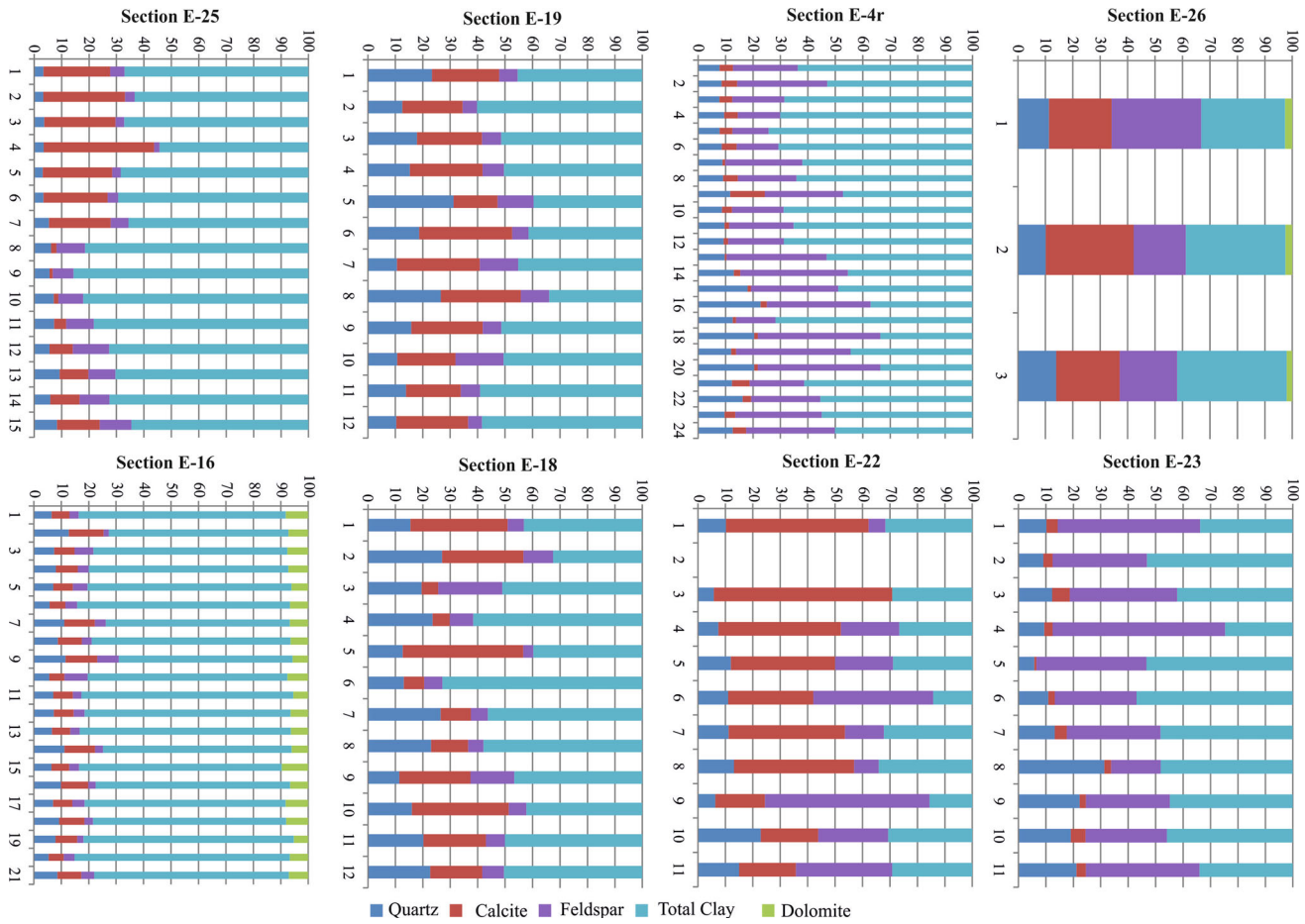

Fig. 6 Bulk mineral composition diagram of the sections E-16, E-18, E-19, E-22, E-23, E-25, E-26 and E-4r (*horizontal axis* is the percentage line; *vertical axis* is the sample numbers line with respect to depth in the column)

conditions; however, between 90 and 210 cm of the section is associated with the increase in total clay amount and apparent decrease in the calcite abundance (Fig. 6). This shows that the sediments within the E-25 section older than 5763 ± 80 cal year BP have experienced relatively humid climate.

In section E-19, from bottom to top, the sediments younger than 6448 ± 29 cal year BP have experienced first relatively dry climate between 140 and 50 cm suggesting from the decrease in total clay abundance associated with increase in the amount of calcite and humid climate between 50 and 0 cm revealing from the increase in clay and decrease in calcite percentages. This is also confirmed with the constant presence of smectite, illite and kaolinite in E-19 section.

Mineralogical abundances of the sediments in E-4r show oscillations throughout the section; however, the general pattern of total clay increases, while calcite decreases relatively from bottom to top of the section. It is suggested that the sediments younger than 11,899 ± 128 cal year BP were deposited in relatively humid climate with high total clay versus much lower calcite amounts. The presence of *Alnus*, *Salix* and decreasing percentages of herbaceous plants especially Chenopodiaceae/Amaranthaceae upwards in the section support this climate change. Having a youngest age in the study area as of 1428 ± 53 cal year BP at E-26-1 sample, the section is proposed to experience relatively drier climates with decreasing total clay and increasing dolomite through the section. The absence of deciduous trees from pollen record of sample E-26-1 is in unison with this climatic interpretation.

Molecular weathering ratios of the sediments around Lakes Eymir and Mogan display trends which are consistent with the mineralogical data. Through the section E-16, almost constant salinization, calcification, clayeyness and base loss are observed, while constant CIA and MAP are also recorded. This implies stable climatic conditions prevailed during the deposition period of E-16 sediments. This is confirmed with the narrow-ranged MAP values between 480 and 512 mm/year. Section E-18 shows apparent oscillations in hydrolyzation, salinization and calcification patterns which are also consistent with its CIA values

(Table S3). Levels in E-18 section corresponding samples of E18-3, 4, 6, 7 and 8 have slightly higher hydrolyzation and low calcification pointing intermediate CIA values which mean relatively higher humidity conditions. This information is also confirmed with the MAP values at the same levels as 916, 919, 933, 939 and 865 mm/year. The field observation of E-22 section shows the disseminated nature of carbonate coating with immature stage of development. This is evidenced by the calcification values generally higher than 2, while hydrolyzation values are relatively low associated with low CIA values (9–36). Generally MAP values are lower than 300 mm/year defining more drier conditions except the lower part of the section where it reaches to 500 mm/year. The deposition of sediments in E-23 section can be directly related to the humid periods since the MAP values through the section are greater than 800 mm/year and also hydrolyzation values >1 with very low degree of calcification.

Cross-plots of $\delta^{13}C$ and $\delta^{18}O$ values show tight clusters with almost no apparent trend for both isotopes for E-16 and E-18 sections. However, good covariance is observed between $\delta^{13}C$ and $\delta^{18}O$ values of the samples from E-4r and E-22 sections. For E-25 samples, there is no apparent trend for $\delta^{18}O$ values; however, approximately 2‰ shift is realized in $\delta^{13}C$ values of the carbonate fractions in the bulk samples (Fig. 7). The absence of covariance between $\delta^{18}O$ and $\delta^{13}C$ values suggests a hydrologically open environment (Talbot 1990). As a general overview on the isotope results, the $\delta^{13}C$ compositions of the samples display relatively wider range than $\delta^{18}O$ which reflects the changing environmental conditions in the fluvio-lacustrine system. The $\delta^{18}O$ values are almost identical and vary within a narrow range reflecting the formation under the influence of meteoric water by medium-elevation precipitation (James and Choquette 1990).

Comparing the $\delta^{13}C$ values of samples with respect to photosynthetic pathways (Cerling and Quade 1993), it is observed that the $\delta^{13}C$ values of the carbonates of this study ranging around −8.6‰ indicate high input of $\delta^{13}C$ from soil respiration and typically correlate with the vegetation cover dominated by C3 plants. However, some depletions in $\delta^{13}C$ may also reflect the seasonal nature of plant activity showing C3:C4 association (Wright and Tucker 1991).

The regular occurrence and abundance of *Pinus* is characteristic of the vegetation at the time of deposition. Although *Pinus* pollen can be abundant because of the capacity of saccate pollen for long-distance transport (Suc and Drivaliari 1991), the considerable presence of it in the studied sections indicates the presence of a coniferous forest. Very high percentages of *Salix* in one of the samples, as a riparian plant, indicate the presence of fluvial conditions in the depositional area. Within the section E-4r, in association with *Pinus* the group of herbs is relatively important in the pollen sum and is mainly made up of Asteraceae/Asteroideae, Asteraceae/Cichorioideae, Chenopodiaceae/Amaranthaceae and Poaceae. This type of vegetation characterizes open areas with herbaceous plants. The open areas within the coniferous forest were mainly occupied by these herbaceous plants. The existence and relative dominance of Chenopodiaceae may indicate the presence of arid conditions. Currently, Chenopodiaceae are common in dry and saline habitats (Kadereit et al. 2005; Marquer et al. 2008). High percentages of herbs within the section E-24 indicate the presence of widespread open areas occupied by herbaceous plants along with coniferous

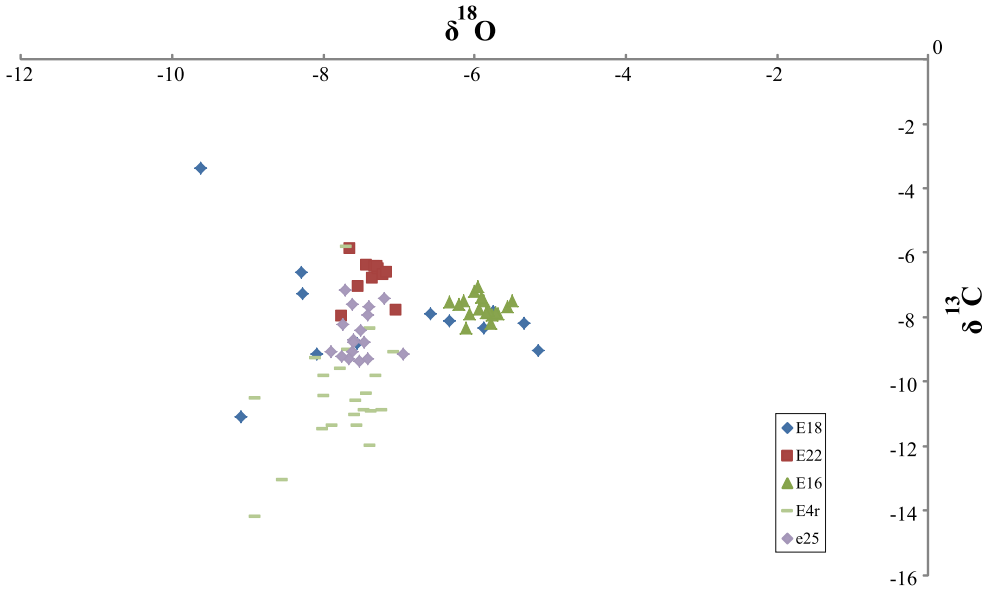

Fig. 7 Cross-plot of $\delta^{13}C$ versus $\delta^{18}O$ compositions of samples from the sections E18, E-16, E-22, E-25 and E-4r

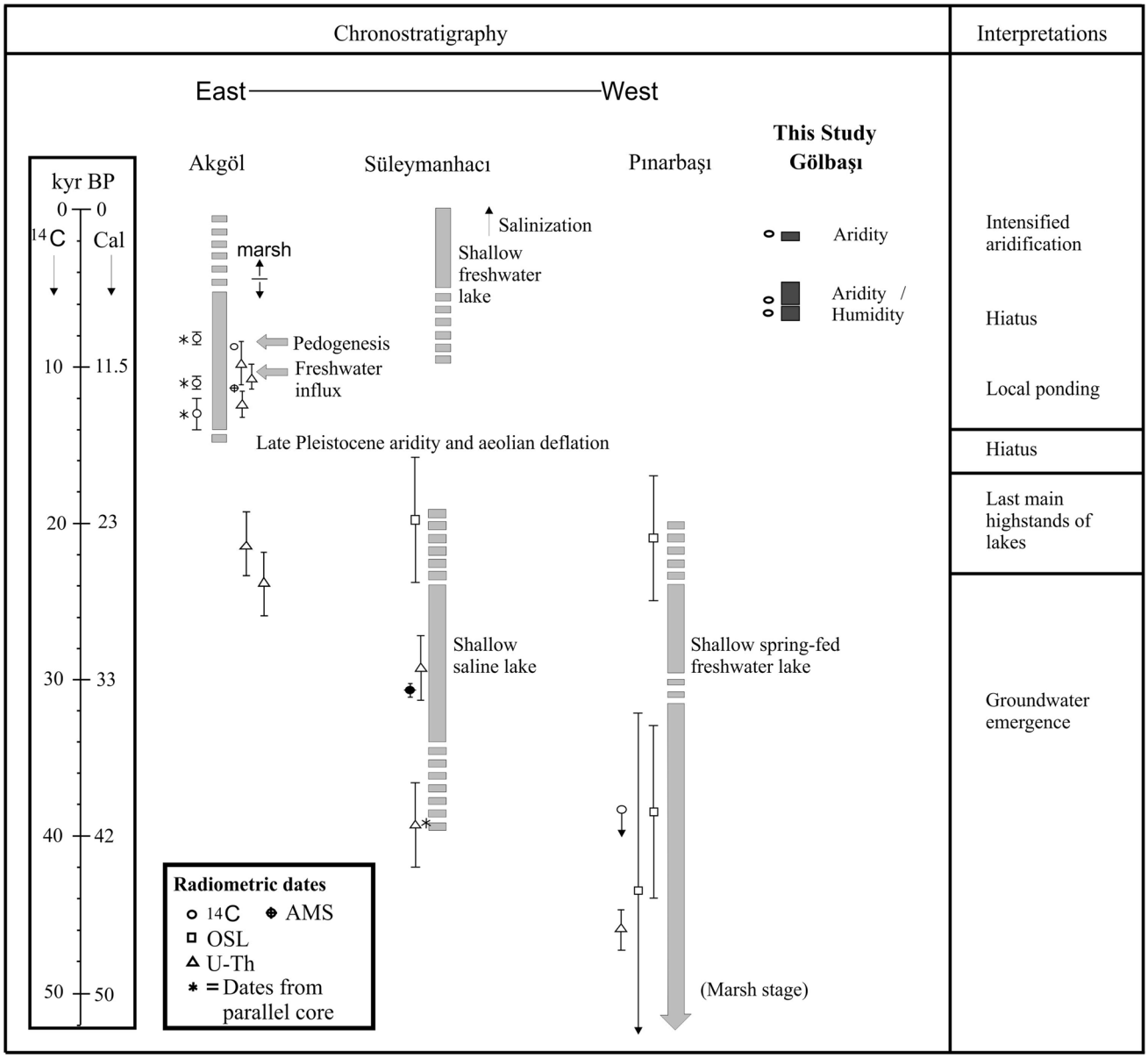

Fig. 8 Chronostratigraphic interpretation of the current findings with the three palaeolake sites in Konya Basin (Nicoll and Küçükuysal 2013 after Roberts et al. 1999)

forests. Dominance of Chenopodiaceae/Amaranthaceae among herbs may reflect relatively dry conditions during deposition of the section E-24. The section E-26 points the presence of a coniferous forest with minor herbs as understory. The identified palynoflora reflects coniferous forests associated with open areas on which Asteraceae and Chenopodiaceae were dominant. Areas covered by herbaceous plants must have been cut away by a river in the shade of *Salix*. This flora may reflect a warm temperate climate.

Overall findings of this study reveal the short climatic history of Gölbaşı (Central Anatolia) between the very Late Pleistocene–Holocene. The first period recorded in the sediments around Lakes Eymir and Mogan is between 11,899 and 6448 cal year BP as dominantly humid time period after Late Pleistocene aridity and aeolian deflation (Roberts et al. 1999). The second period recorded is between 6448 and 5763 cal year BP corresponding to intercalating dry and wet conditions. The last period between 5763 and 1428 cal year BP is recorded as dominantly low precipitation–dry conditions associated with less intense humid pulses which led to the formation of palaeosols in the study area. These findings have consistency with the coeval proxy records of Roberts et al. (1999) in Konya Plain (Fig. 8). The time range of 11,899–6448 cal year BP overlaps with the "local

ponding + freshwater influx" period (Nicoll and Küçükuysal 2013; Roberts et al. 1999), while the second recorded period of 6448–5763 cal year BP falls in the "pedogenesis" event (Roberts et al. 1999) which requires mostly humidity associated scarce dryness. The last recorded time range of this study, 5763–1428 cal year BP, coincides with the intensified aridity (Nicoll and Küçükuysal 2013; Roberts et al. 1999). The rapid climate changes or RCCs (Mayewski et al. 2004) are also compared with the current findings that RCCs of 6000–5000 and 1200–1000 cal year BP indicate the pronounced aridity which is also obtained from the recent findings of this study.

Conclusions

As a result of these above interpretations, it can be concluded that the mineralogical, geochemical, palynological and stable isotopic compositions of the Late Pleistocene–Holocene fluvio-lacustrine sediments around Lakes Eymir and Mogan (Ankara), Central Anatolia, provide multi-proxy data to infer the palaeoclimates and palaeovegetation between 11,899 and 1428 cal year BP. The period between 11,899 and 6448 cal year BP was rather humid interval within the Holocene. Subsequent to this period, humidity became insufficient but was intercalated with dryness between 6448 and 5763 cal year BP. The last period of 5763–1428 cal year BP is realized with its aridity.

Acknowledgements This study was supported financially by the General Directorate of Mineral Research and Exploration under Project No. 2012-30-14-08-3. The invaluable contribution to the field study from Emre Şimşek and Zeynep Arı is appreciated. The authors are especially grateful to the editor and anonymous reviewers for their careful and constructive comments which significantly improved the quality of the manuscript.

References

Akyürek B (1981) Fundamental geological characteristics of northern part of Ankara melange. In: Symposium on Central Anatolia. Geological Society Turkey, pp 41–52 **(in Turkish)**

Akyürek B, Bilginer E, Dağer Z, Sunu O (1979a) The occurrence of the Lower Triassic of the Hacılar (N of Çubuk-Ankara). Bull Geol Soc Turk 22:169–174 **(in Turkish)**

Akyürek B, Bilginer E, Dağer Z, Soysal Y, Sunu O (1979b) Evidences for the ophiolite emplacement around Eldivanli–Şabanözü. Chamb Geol Eng 9:5–11 **(in Turkish)**

Akyürek B, Bilginer E, Çatal E, Dağer Z, Soysal Y, Sunu O (1980) Geology of the Eldivan–Şabanözü (Çankırı) and Hasayaz–Çandır (Kalecik–Ankara) regions. MTA Report no:6741 **(in Turkish-unpublished)**

Akyürek B, Duru M, Sütçü YF, Papak İ, Şaroğlu F, Pehlivan N, Gönenç O, Granit S, Yaşar T (1997) 1: 100000 Scale Geological Maps of Turkey, No: 55, Ankara F-15 Sheet. General Directorate of Mineral Research and Exploration, Ankara **(in Turkish)**

Altin TB, El Ouahabi M, Fagel N (2015) Environmental and climatic changes during the Pleistocene–Holocene in the Bor Plain, Central Anatolia, Turkey. Palaeogeogr Palaeoclimatol Palaeoecol 440:564–578

Arıkan B (2015) Modeling the paleoclimate (ca. 6000–3200 cal BP) in eastern Anatolia: the method of Macrophysical Climate Model and comparisons with proxy data. J Archaeol Sci 57:158–167

Benito G, Macklin MG, Zielhofer C, Jones AF, Machado MJ (2015) Holocene flooding and climate change in the Mediterranean. Catena 130:13–33

Biltekin D, Popescu S, Suc J, Quézel P, Jiménez-Moreno G, Yavuz N, Çağatay MN (2015) Anatolia: a long-time plant refuge area documented by pollen records over the last 23 million years. Rev Palaeobot Palynol 215:1–22

Biscaye PE (1965) Mineralogy and sedimentation of recent deep-sea clay in the Atlantic Ocean and adjacent seas and oceans. Geol Soc Am Bull 76:803–832

Bischoff JL, Cummins K (2001) Wisconsin glaciation of the Sierra Nevada (79,000–15,000 yr BP) as recorded by rock $our in sediments of Owens Lake, California. Quat Res 55:14–24

Brindley GW (1980) Quantitative analysis of clay mixtures. In: Brindley GW, Brown G (eds) Crystal structures of clay minerals and their X-ray identification. Monograph 5. Mineralogical Society, London, pp 411–438

Candy I, Black S, Sellwood BW, Rowan JS (2003) Calcrete profile development in Quaternary alluvial sequences, southeast Spain: implications for using calcretes as a basis for landform chronologies. Earth Surf Process Landf 28:169–185

Cerling TE, Quade J (1993) Stable carbon and oxygen isotopes in soil carbonates. In: Swart PK, Lohmann KC, McKenzie JA, Savin SM (eds) Climate change in continental isotopic records. Geophysical Monograph, vol 78. American Geophysical Union, Washington, pp 217–231

Çiner A (2004) Turkish glaciers and glacial deposits. In: Ehlers J, Gibbard PL (eds) Quaternary glaciations: extent and chronology, part 1: Europe. Elsevier, Amsterdam, pp 419–429

Deutz P, Montanez IP, Monger HC (2001) Morphology and isotope heterogeneity of Late Quaternary pedogenic carbonates: implications for paleosol carbonates as paleoenvironmental proxies. Palaeogeogr Palaeoclimatol Palaeoecol 166:293–317

Diekmann B, Hofmann J, Henrich R, Fütterer DK, Röhl U, Wei K (2008) Detrital sediment supply in the southern Okinawa Trough and its relation to sea-level and Kuroshio dynamics during the late Quaternary. Mar Geol 255:83–95

Doğan U (2010) Fluvial response to climate change during and after the Last Glacial Maximum in Central Anatolia, Turkey. Quat Int 222:221–229

Doğan U (2011) Climate-controlled river terrace formation in the Kızılırmak Valley, Cappadocia section, Turkey: inferred from Ar–Ar dating of Quaternary basalts and terraces stratigraphy. Geomorphology 126:66–81

Eastwood WJ, Roberts N, Lamb HF, Tibby JC (1999) Holocene environmental change in southwest Turkey: a palaeoecological record of lake and catchment-related changes. Quat Sci Rev 18:671–696

Eren M, Kadir S, Hatipoğlu Z (2008) Quaternary calcrete development in the Mersin Area, southern Turkey. Turk J Earth Sci 17:763–784

Eriş KK (2013) Late Pleistocene–Holocene sedimentary records of climate and lake-level changes in Lake Hazar, eastern Anatolia, Turkey. Quat Int 302:123–134

Faegri K, Iversen J (1989) Textbook of pollen analysis. Wiley, Chichester

Göktürk OM, Fleitmann D, Badertsscher S, Cheng H, Edwards RL, Leuenberger M, Fankhauser A, Tüysüz O, Kramers J (2011) Climate on the southern Black Sea coast during the Holocene:

implications from the Sofular Cave record. Quat Sci Rev 30:2433–2445
Göz E, Kadir S, Gürel A, Eren M (2014) Geology, mineralogy, geochemistry, and depositional environment of a Late Miocene/Pliocene fluviolacustrine succession, Cappadocian Volcanic Province, Central Anatolia, Turkey. Turk J Earth Sci 23:386–411
Grimm EC (2005) TILIA and TILIA Graph. PC spreadsheet and graphics software for pollen data. Illinois State Museum, Springfield
Gündoğdu MN (1982) Neojen yaşlı Bigadiç sedimanter baseninin jeolojik, mineralojik ve jeokimyasal incelenmesi, Ph.D. Thesis. Hacettepe Univeristy (unpublished), Ankara
Jackson ML (1979) Soil chemical analysis-advanced course, 2nd edn. Published by the Author, Madison, p 895
Jalut G, Dedoubat JJ, Fontugne M, Otto T (2009) Holocene circum-Mediterranean vegetation changes: climate forcing and human impact. Quat Int 200:4–18
James NP, Choquette PW (1990) Diagenesis-9: limestones: the meteoric diagenetic environment. In: McIlreath IA, Morrow DW (eds) Diagenesis. Ottawa. Geoscience Canada Reprint Series 4, pp 35–73
Jason R, Price JR, Velbel MA, Patino LC (2005) Rates and time scales of clay-mineral formation by weathering in saprolitic regoliths of the southern Appalachians from geochemical mass balance. Bull Geol Soc Am 117:783–794
Jones MD, Roberts CN, Leng MJ, Türkes M (2006) A highresolution late Holocene Lake isotope record from Turkey and links to North Atlantic and monsoon climate. Geology 43:361–364
Kadereit G, Gotzek D, Jacobs S, Freitag H (2005) Origin and age of Australian Chenopodiaceae. Org Divers Evol 5:59–80
Kadir S, Gürel A, Senem H (2013) Geology of Late Miocene clayey sediments and distribution of palaeosol clay minerals in the northeastern part of the Cappadocian Volcanic Province (Araplı–Erdemli), Central Anatolia, Turkey. Turk J Earth Sci 22:427–443
Karabiyikoğlu M, Kuzucuoğlu C, Fontugne M, Kaiser B, Mouralis D (1999) Facies and depositional sequences of the Late Pleistocene Göçü shoreline system, Konya basin, Central Anatolia: implications for reconstructing lake-level changes. Quat Sci Rev 18:593–609
Kazancı N, Leroy SAG, Ileri Ö, Emre Ö, Kibar M, Öncel S (2004) Late Holocene erosion in NW Anatolia from sediments of Lake Manyas, Lake Ulubat and the southern shelf of the Marmara Sea, Turkey. Catena 57:277–308
Kazancı N, Boyraz S, Özkul M, Alçiçek MC, Kadıoğlu YK (2012) Late Holocene terrestrial tephra record at western Anatolia, Turkey: possible evidence of an explosive eruption outside Santorini in the eastern Mediterranean. Glob Planet Change 80–81:36–50
Kotthoff U, Müller UC, Pross J, Schmiedl G, Van De Schootbrugge B, Lawson I, Schulz H (2008) Lateglacial and Holocene vegetation dynamics in the Aegean region: an integrated view based on pollen data from marine and terrestrial archives. Holocene 18:1019–1032
Kovacs J, Raucsik B, Varga A, Ujvarı G, Varga G, Ottner F (2013) Clay mineralogy of red clay deposits from the Central Carpathian Basin (Hungary): implications for Plio–Pleistocene chemical weathering and paleoclimate. Turk J Earth Sci 22:414–426
Küçükuysal C (2011) Palaeoclimatological approach to Plio-Quaternary paleosol-calcrete sequences in Bal and Gölba l (Ankara) by using mineralogical and geochemical proxies. METU PhD Thesis, Middle East Technical University, Ankara, pp 1—246
Küçükuysal C (2016) Late Pleistocene calcretes from Central Anatolia (Lake Eymir and Mogan, Gölbaşı Basin): comparison to quaternary calcretes from Turkey. J Earth Sci 27:874–882
Küçükuysal C, Kapur S (2014) Mineralogical, geochemical and micromorphological evaluation of the Plio-Quaternary paleosols and calcretes from Karahamzalı, Ankara (Central Turkey). Geol Carpath 65:241–253
Küçükuysal C, Türkmenoğlu AG, Kapur S (2013) Multi-proxy evidence of Mid-Pleistocene dry climates observed in calcretes in Central Turkey. Turk J Earth Sci 22:463–483
Kuzucuoğlu C, Karabıyıkoğlu M, Parish R (1998) The dune systems of the Konya Plain (Turkey). Their relation to the environmental changes in Central Anatolia during Late Pleistocene and Holocene. Geomorphology 23:257–271
Kuzucuoğlu C, Dörfler W, Kunesch S, Goupille F (2011) Mid- to late-Holocene climate change in central Turkey: the Tecer Lake record. Holocene 21:173–188
Landmann G, Reimer A, Kempe S (1996) Climatically induced lake level changes at Lake Van, Turkey, during the Pleistocene/Holocene transition. Glob Biogeochem Cycles 10:797–808
Marquer L, Pomel S, Abichou A, Schulz E, Kaniewski D, Van Campo E (2008) Late Holocene high resolution palaeoclimatic reconstruction inferred from Sebkha Mhabeul, southeast Tunisia. Quat Res 70:240–250
Martins V, Rocha F, Sequeira C, Martins P, Santos J, Dias JA, Weber O, Jouanneau J, Rubio B, Rey D, Bernabeu A, Silva E, Laut L, Figueira R (2013) Late Holocene climatic oscillations traced by clay mineral assemblages and other palaeoceanographic proxies in Ria de Vigo (NW Spain). Turk J Earth Sci 22:398–413
Mauri A, Davis BAS, Collins P, Kaplan J (2015) The climate of Europe during the Holocene: a gridded pollen-based reconstruction and its multi-proxy evaluation. Quat Sci Rev 112:109–127
Mayewski PA, Rohling EE, Stager JC, Karlén W, Maasch KA, Meeker LD, Meyerson EA, Gasse F, Van Kreveld S, Holmgren K, Lee-Thorp J, Rosqvist G, Rack F, Staubwasser M, Schneider RR, Steig EJ (2004) Holocene climate variability. Quat Res 62:243–255
Moore DM, Reynolds JR (1989) X-ray diffraction and the identification and analysis of clay minerals. Oxford University Press, Oxford
Moore DM, Reynolds RC Jr (1997) X-ray diffraction and the identification and analysis of clay minerals. Oxford University Press, Oxford
Moore P, Webb J, Collinson M (1991) Pollen analysis, 2nd edn. Blackwell, Oxford
Nicoll K, Küçükuysal C (2013) Emerging multi-proxy records of Late Quaternary Palaeoclimate dynamics inTurkey and the surrounding region. Turkish J Earth Sci 22:126–142
Ocakoğlu F, Kır O, Yılmaz İÖ, Açıkalın S, Erayık C, Tunoğlu C, Leroy SAG (2013) Early to Mid-Holocene Lake level and temperature records from the terraces of Lake Sünnet in NW Turkey. Palaeogeogr Palaeoclimatol Palaeoecol 369:175–184
Oehlert AM, Swart PK (2014) Interpreting carbonate and organic carbon isotope covariance in the sedimentary record. Nat Commun 5:4672. doi:10.1038/ncomms5672
Peyron O, Dormoy I, Kotthoff U, Pross J, De Beaulieu J-L, Drescher-Schneider R, Magny M (2011) Holocene seasonality changes in the central Mediterranean region reconstructed from the pollen sequences of Lake Accesa (Italy) and Tenaghi Philippon (Greece). Holocene 21:131–146
Rabenhorst MC, West LT, Wilding LP (1991) Genesis of calcic and petrocalcic horizons in soils over carbonate rocks. In: Nettleton WD (ed) Occurrence, characteristics and genesis of carbonate, gypsum and silica accumulations in soils SSSA Special publication number 26. Soil Science Society of America, Inc., Madison, pp 61–74
Reille M (1992) Pollen et Spores D' Europe et D'Afrique du Nord. Marseille, France, 520 p

Retallack GJ (1997) A colour guide to paleosols. Wiley, Chichester, p 188

Retallack GJ (2001) Soils of the past. Blackwell, Oxford, p 600

Roberts CN (1983) Age, palaeoenvironments, and climatic significance of late Pleistocene Konya Lake, Turkey. Quat Res 19:154–171

Roberts N, Wright HE Jr (1993) Vegetational, lake level and climatic history of the Near East and Southwestern Asia. In: Wright HE Jr, Kutzbach JE, Webb IT II, Ruddiman WF, Street-Perrot FA, Bartlein PJ (eds) Global climates since the last glacial maximum. University of Minnesota Press, Minneapolis, pp 53–67

Roberts N, Black S, Boyer P, Eastwood WJ, Griffiths HI, Lamb HF, Leng MJ, Parish R, Reed JM, Twigg D, Yiğitbaşioğlu H (1999) Chronology and stratigraphy of late Quaternary sediments in the Konya basin, Turkey: results from the KOPAL project. Quaternary Sci Rev 18:611–630

Roy PD, Caballero M, Lozano R, Pi T, Morton O (2009) Late Pleistocene–Holocene geochemical history inferred from Lake Tecocomulco sediments, Basin of Mexico, Mexico. Geochem J 43:49–64

Şenkul Ç, Doğan U (2013) Vegetation and climate of Anatolia and adjacent regions during the last glacial period. Quaternary Int 302:110–122

Sheldon ND, Tabor NJ (2009) Quantitative paleoenvironmental and paleoclimatic reconstruction using paleosols. Earth Sci Rev 95:1–52

Sheldon ND, Retallack GJ, Tanaka S (2002) Geochemical climofunctions from North American soils and application to paleosols across the Eocene–Oligocene boundary in Oregon. J Geol 110:687–696

Staubwasser M, Weiss H (2006) Holocene climate and cultural evolution in late prehistoric–early historic West Asia. Quat Res 66:372–387

Stuchlik L (1994) Neogene pollen flora of Central Europe, Part 1. Acta Paleobotanica, Supplementum No. 1, Krakow

Suc J-P, Drivaliari A (1991) Transport of bisaccate coniferous fossil pollen grains to coastal sediments: an example from the earliest Pliocene orb Ria (Languedoc, Southern France). Rev Palaeobot Palynol 70:247–253

Talbot MR (1990) A review of the paleohydrological interpretation of carbon and oxygen isotopic ratios in primary lacustrine carbonates. Chem Geol (Isotope Geosci Sect) 80:26179

Tamban M, Purnachandra Rao V, Schneider RR (2002) Reconstruction of late quaternary monsoon oscillations based on clay mineral proxies using sediment cores from the western margin of India. Mar Geol 186:527–539

Thorez J (1976) Practical identification of clay minerals. Lelotte, Dison, p 89

Tucker M (1988) Techniques in sedimentology. Blackwell Scientific Publications, Oxford, p 394

Ülgen UB, Franz OS, Biltekin D, Çağatay NM, Roeser AP, Doner L, Thein J (2012) Climatic and environmental evolution of Lake Iznik (NW Turkey) over the last ~4700 years. Quat Int 274:88–101

Veldkamp A, Candy I, Jongmans AG, Maddy D, Demir T, Schoorl JM, Schreve D, Stemerdink C, van der Schriek T (2015) Reconstructing Early Pleistocene (1.3 Ma) terrestrial environmental change in western Anatolia: did it drive fluvial terrace formation? Palaeogeogr Palaeoclimatol Palaeoecol 417:91–104

Verrecchia EP, Freytet P, Verrecchia KE, Dumont JL (1995) Spherulites in calcrete laminar crusts: biogenic $CaCO_3$ precipitation as a major contributor to crust formation. J Sediment Res 65:690–700

Wagner S, Guenster N, Skowronek A (2012) Genesis and climatic interpretation of paleosols and calcretes in a Plio-Pleistocene alluvial fan of the Costa Blanca (SE Spain). Quat Int 265:170–178

Wick L, Lemcke G, Sturm M (2003) Evidence of late glacial and Holocene climatic change and human impact in eastern Anatolia: high-resolution pollen, charcoal, isotopic and geochemical records from the laminated sediments of Lake Van, Turkey. Holocene 13:665–675

Wright VP, Tucker ME (1991) Calcretes. Blackwell Science Scientific Publications, Oxford, p 351

Yağbasan Ö (2007) Modelling of Mogan and Eymir lakes aquifer system, Ph.D. dissertation. Middle-East Technical University, p 163

Yavuz N, Culha G, Demirer ŞS, Utescher T, Aydın A (2016) Pollen, ostracod and stable isotope records of palaeoenvironment and climate: Upper Miocene and Pliocene of the Çankırı Basin (Central Anatolia, Turkey). Palaeogeogr Palaeoclimatol Palaeoecol. doi:10.1016/j.palaeo.2016.04.023

Yuretich R, Ervin C (2002) Clay minerals as paleoenvironmental indicators in two large lakes of the African Rift Valleys: Lake Malawi and Lake Turkana. In: Renaut RW, Ashley GM (eds) Sedimentation in continental rifts, vol 73, pp 221–232